

Restoration of Movement and Apical Growth in the Angiosperm Pollen Tube Following Cytochalasin-Induced Paralysis

J. Heslop-Harrison and Y. Heslop-Harrison

Phil. Trans. R. Soc. Lond. B 1991 **331**, 225-235
doi: 10.1098/rstb.1991.0011

Email alerting service

Receive free email alerts when new articles cite this article - sign up in the box at the top right-hand corner of the article or click [here](#)

Restoration of movement and apical growth in the angiosperm pollen tube following cytochalasin-induced paralysis

J. HESLOP-HARRISON AND Y. HESLOP-HARRISON

Institute of Grassland and Ecological Research, University College of Wales, Plas Gogerddan, Aberystwyth SY23 3EB, U.K.

SUMMARY

Cytochalasin D (CD) at $5 \mu\text{g ml}^{-1}$ arrested growth and vectorial movement in pollen tubes of *Narcissus pseudonarcissus* and *Endymion nonscriptus* and caused the mainly longitudinally oriented actin fibrils in the vegetative cells to coalesce and form massive, more randomly oriented, cables. As extension growth was arrested, the tubes formed apical bulbs and abnormal wall thickenings. During recovery from a 10 min treatment period in *E. nonscriptus*, an essentially normal fibril system was reconstituted by partial dissociation of the thick cables formed during the exposure to CD. As this progressed movement was restored in the vegetative cells. Some 80% of the blocked tubes initiated new growing points, either by producing randomly oriented swellings in sites where the wall was thinner, or by erosion and penetration of thicker zones. Contrary to expectation, the sites of the prospective growing points were not indicated in advance by any special disposition of the actin cytoskeleton. With the transition to cylindrical growth in the secondary tubes the standard stratification of the tube wall reappeared, with outer pectocellulosic and inner callosic layers. Normal movement pathways were established concomitantly, together with the apical zonation of organelles and other cytoplasmic inclusions characteristic of the extending tube. CD-treatment brought about rapid contraction of the vegetative nuclei with the loss of the elastic extensions of the nuclear envelopes. The extended form was resumed as the actin cytoskeleton was restored during recovery, and vegetative nuclei and generative cells moved into the secondary tubes where they continued to track the apex as in the normal tube.

1. INTRODUCTION

Franke *et al.* (1972) and Mascarenhas & Lafountain (1972) reported that the cytochalasins, heterocyclic fungal metabolites, inhibit extension growth and the movement of organelles and other cytoplasmic inclusions in angiosperm pollen tubes, and that the effects are reversed when the tubes are restored to a normal growth medium. Movement in the pollen tube, like that in various other plant cells (reviews, Williamson 1986; Staiger & Schliwa 1987), is based on an actomyosin system, and the weight of the current evidence supports the view that the target of cytochalasin action in the vegetative cell is the actin cytoskeleton. Cytochalasin effects in animal cells, including the inhibition of locomotion, intracellular movement and various morphogenetic processes are also generally reversible (Wessels *et al.* 1971). However, in many instances the restoration to a state approaching normal is relatively slow, occupying even hours (e.g., in cultured HeLa cells, see Miranda *et al.* (1974)). The recovery in the pollen tube is, in contrast, remarkably quick. Thus in the distal stretches of tubes of *Iris* exposed to cytochalasin B for 15 min, vectorial movement of even the larger bodies recommenced in less than 60 s from exposure to suitable cytochalasin-

free medium (Heslop-Harrison & Heslop-Harrison 1989a), although in the older, proximal parts of the tube, sustained, long-range cyclosis was never restored. Instead, the cytoplasm fragmented to form detached masses which underwent irregular amoeboid movement, with organelles moving rapidly in random trajectories.

Currently, the biochemical evidence does not offer any unequivocal guide to what might be expected from cytochalasin action in living cells, or to what might be involved in recovery. Reviewing the current state of knowledge, Cooper (1987) states that the surest conclusion is that the cytochalasins cap the growing, barbed, ends of actin filaments, preventing further extension. While dismissing the view that cytochalasins depolymerize actin filaments, this author nevertheless accepts the possibility that they might cause breakage by binding to subunits in the interior of a filament. Yet the fact that at least in some cases a functional motility system is regenerated very rapidly necessarily implies that the actin cytoskeleton is not broken up or otherwise drastically impaired by cytochalasin treatment. That individual actin microfilaments are not disrupted by the cytochalasins, at least *in vitro*, is shown by the earlier results of Forer *et al.* (1972), who found that F-actin filaments prepared from rabbit muscle G-

actin survived exposure to cytochalasin B at the high concentration of 0.5 mg ml^{-1} without structural modification. Interpretations of the actual effect on the actin microfilament system of the living cells have been quite diverse: in some instances no modifications of ultrastructure have been observed (Bradley 1973), while in others condensation of the microfilaments towards local foci, or association to form felt-like, ribbon-like or rod-like aggregates have been reported (Schliwa 1982; Miranda *et al.* 1974; Rathke *et al.* 1977).

A recent paper by Lancelle & Hepler (1988) has provided details of one conspicuous effect of the cytochalasins on the pollen tubes of *Nicotiana glauca*. These authors used rapid freeze-fixation followed by freeze-substitution to prepare cytochalasin-treated tubes for electron microscopy, a procedure generally held to conserve cytoplasmic structure more effectively than standard methods of chemical fixation. Cytochalasins B and D were each found to cause the microfilaments of the vegetative cell to aggregate in massive, randomly oriented bundles. Micrographs of longitudinally sectioned microfilament bundles in pollen tubes prepared in this way show widths of $0.5 \text{ }\mu\text{m}$ or more. These bundles were evidently quite similar to the actin aggregates present in ungerminated pollen grains (Cresti *et al.* 1986; Heslop-Harrison *et al.* 1986), which dissociate progressively during activation and germination to produce the extended fibril system of the pollen tube (Heslop-Harrison & Heslop-Harrison 1989*b*).

In the present paper we report on an investigation of the effects of cytochalasin D on the actin cytoskeleton of pollen tubes of *Narcissus pseudonarcissus*, and on the events associated with the restoration of intracellular movement and the regeneration of the tip-growth system in tubes of *Endymion nanscriptus* following temporary cytochalasin-induced paralysis. We have used fluorochrome-coupled phalloidin as a label for actin fibrils, with a preparation method similar to that first introduced for pollen tubes by Pierson (1988) using direct permeabilization and avoiding chemical fixation. This method reveals details of the fibril system of the pollen tube comparable with those seen in favourable zones of living tubes (Heslop-Harrison & Heslop-Harrison 1988), and also compatible with the images obtained from electron microscopy of microfilament cables in freeze-substituted pollen tubes (Lancelle *et al.* 1988).

2. MATERIALS AND METHODS

The observations were made on a cultivar of *Narcissus pseudonarcissus* L. and on *Endymion nanscriptus* (L.) Garcke from a natural population in west Wales. The greater diameter of the pollen tubes of *N. pseudonarcissus* made this species suitable for tracing the effects of cytochalasin on the actin cytoskeleton, but the lower pollen fertility of the cultivar used, 50–60%, meant that it was less suitable for comparative studies. Accordingly the main experiments were carried out with *E. nanscriptus*, which, while producing narrower tubes, regularly showed pollen fertility of 80–95%.

Pollen from freshly dehiscing anthers was germinated and grown in aqueous media (GM) containing $1 \text{ mM Ca(NO}_3)_2$, $1 \text{ mM H}_3\text{BO}_3$, with 15% sucrose for *E. nanscriptus* and 7.5% sucrose for *N. pseudonarcissus*. To ensure maximum reproducibility and consistency of tube growth in the cultures of *E. nanscriptus* before the beginning of treatment, each sample, approximately equivalent to the pollen yields of 18 anthers, was dispersed with a vibrator in 2.5 ml GM in a 10 ml glass vial, and aerated continuously thereafter on a rotator at 22–24 °C.

Cytochalasin D (CD) was dissolved in dimethylsulphoxide (DMSO) at a concentration of 1 mg ml^{-1} , and aliquots added to portions of GM to give a final concentration of $5 \text{ }\mu\text{g ml}^{-1}$. There were no discernible effects on growth rate or tube form in controls run with corresponding concentrations of DMSO alone.

Samples for treatment were withdrawn from pollen cultures of the ages required and pipetted into microcentrifuge tubes. The pollen tubes were then concentrated by low speed centrifugation, drained free of GM, and rapidly dispersed in the treatment medium in the same microcentrifuge tubes before being returned to the rotator. After the desired intervals the samples were concentrated once more, drained, washed once in GM and suspended in fresh GM for further culture, again in the same tubes. Each transfer occupied 150–210 s.

For observation of living tubes small samples of the suspensions were withdrawn and transferred to glass cells on the microscope stage. Continuous video recordings of events in individual tubes were made with differential interference (DIC) optics, and the movements of inclusions and the changes in the cytoplasm during CD treatment and subsequent recovery were analysed from the videotapes as previously described (Heslop-Harrison & Heslop-Harrison 1987, 1988). Photomicrographs of living tubes were also made with extended exposures of 3–8 s. Such 'streak' micrographs allow those inclusions moving in the cytoplasm at the time to produce blurred images polarized in the direction of travel, helping to define the sites and limits of the principal traffic pathways in the tube (Heslop-Harrison & Heslop-Harrison 1988, 1990*a*).

Samples for localizing pollen tube wall components were fixed at room temperature for about 3 h in 2.5% glutaraldehyde in 0.05 M phosphate buffer with 10% sucrose, and stained as follows: calcofluor white (CFW), 0.001% in 10% sucrose as a fluorochrome for cellulosic glucans; aniline blue, 0.05% in 10% sucrose decolorized at pH 11 as a fluorochrome for callose, and alcian blue 8GX, *ca.* 1% in 3% acetic acid, for pectic polysaccharides. The specificity of these stains has been discussed in an earlier paper, where pertinent literature is cited (Heslop-Harrison & Heslop-Harrison 1985). Lipid inclusions were identified by staining with scarlet R saturated in 50% ethanol, and vegetative cell and generative cell nuclei were localized with the DNA-specific fluorochrome 4,6-diamidino-2-phenylindole (DAPI) at approximately 0.0005% aqueous (Heslop-Harrison & Heslop-Harrison 1984). Mitochondria were identified in living tubes of *E. nanscriptus* with the fluorochrome 3,3'-diethyl-oxacarbocyanine

iodide at $0.5 \mu\text{m l}^{-1}$ as described elsewhere (Heslop-Harrison et al. 1990*a,b*). Dimensions were measured with a microcomputer, digitizer and camera lucida system.

Phalloidin labelled with tetramethyl-rhodamine B isothiocyanate (Tr-Ph; Sigma) was used for localizing actin fibrils. The tracer was dissolved in methanol at 0.05 mg ml^{-1} and taken up immediately before use in 0.05 M phosphate buffer at pH 6.8 with 4% mannitol and 5% DMSO so as to give a final concentration of $1 \mu\text{g ml}^{-1}$. Droplets of the pollen cultures (*ca.* $200 \mu\text{l}$) were dispersed on poly-L-lysine coated slides, drained free of GM, rinsed with buffered mannitol and flooded with $200 \mu\text{l}$ of the Tr-Ph medium. Coupling was accelerated by irradiation for 5–10 s in a 500W microwave oven. The samples were then drained of the medium, cooled by flooding with buffered mannitol and prepared for observation. Micrographs were made on Ilford XP1 film rated at a nominal 1600 ASA.

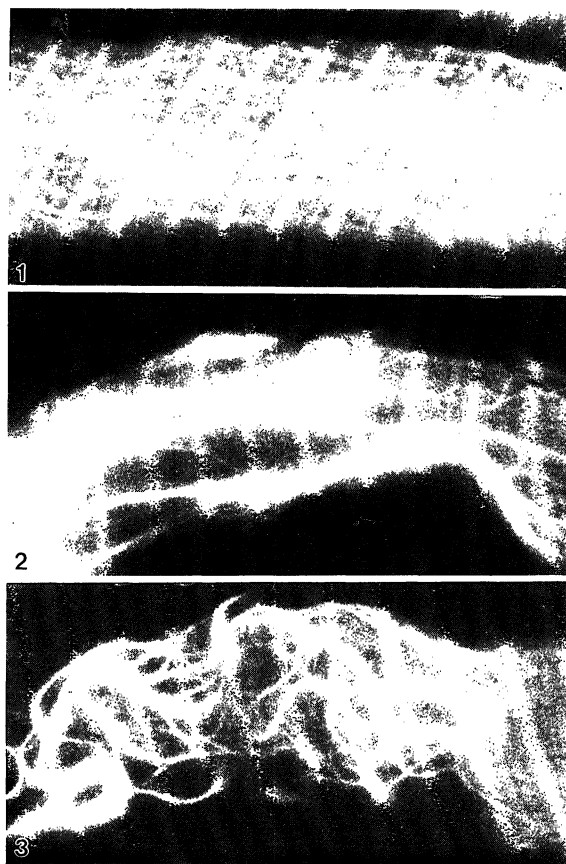
3. RESULTS

(a) Effects of CD on the actin cytoskeleton of pollen tubes of *N. pseudonarcissus*

Figure 1 shows the actin cytoskeleton of a segment of a pollen tube of *N. pseudonarcissus* proximal to the apex, as revealed by Tr-Ph staining. The actin fibrils are disposed mainly longitudinally in this part of the tube, where individual fibrils can often be traced uninterruptedly for more than $100 \mu\text{m}$ along the length. There are occasional inversions and apparent anastomoses, but few indications of lateral fusion. Exposure to CD induces rapid and dramatic change. The micrograph of figure 2 is from a segment of a tube corresponding approximately to that of figure 1 and subjected after CD treatment to Tr-Ph staining in an identical manner. In this part of the tube most of the original fibrils have become apposed to produce cables of various widths, while retaining an overall longitudinal disposition. In figure 3, of a segment of a tube in the vicinity of the vegetative nucleus, the fibrils have again associated laterally to form thicker strands, but in this zone they have evidently contracted somewhat along the length of the tube, coiling in consequence. While figures 2 and 3 show what is undoubtedly a frequent response to CD, namely apposition of the original slender actin fibrils to form thicker cables, the fibrils appeared to be fragmented in parts of some otherwise seemingly undamaged tubes of *N. pseudonarcissus* prepared for Tr-Ph staining in the same manner.

(b) Events associated with recovery from CD-induced arrest

Figure 4 shows the state of the actin cytoskeleton in a sub-apical zone of a 45 min pollen tube of *E. nonscriptus* before CD treatment. As in the corresponding part of *N. pseudonarcissus* tubes, the slender fibrils are oriented mainly longitudinally. Continuous video records showed that sustained vectorial movement of organelles, generative cells and vegetative nuclei ceased within 70–80 s from transfer to the CD



Figures 1–3. Unfixed pollen tubes of *Narcissus pseudonarcissus* *ca.* 70 min from initial hydration in GM, Tr-Ph staining. (Magn. $\times ca.$ 2173.)

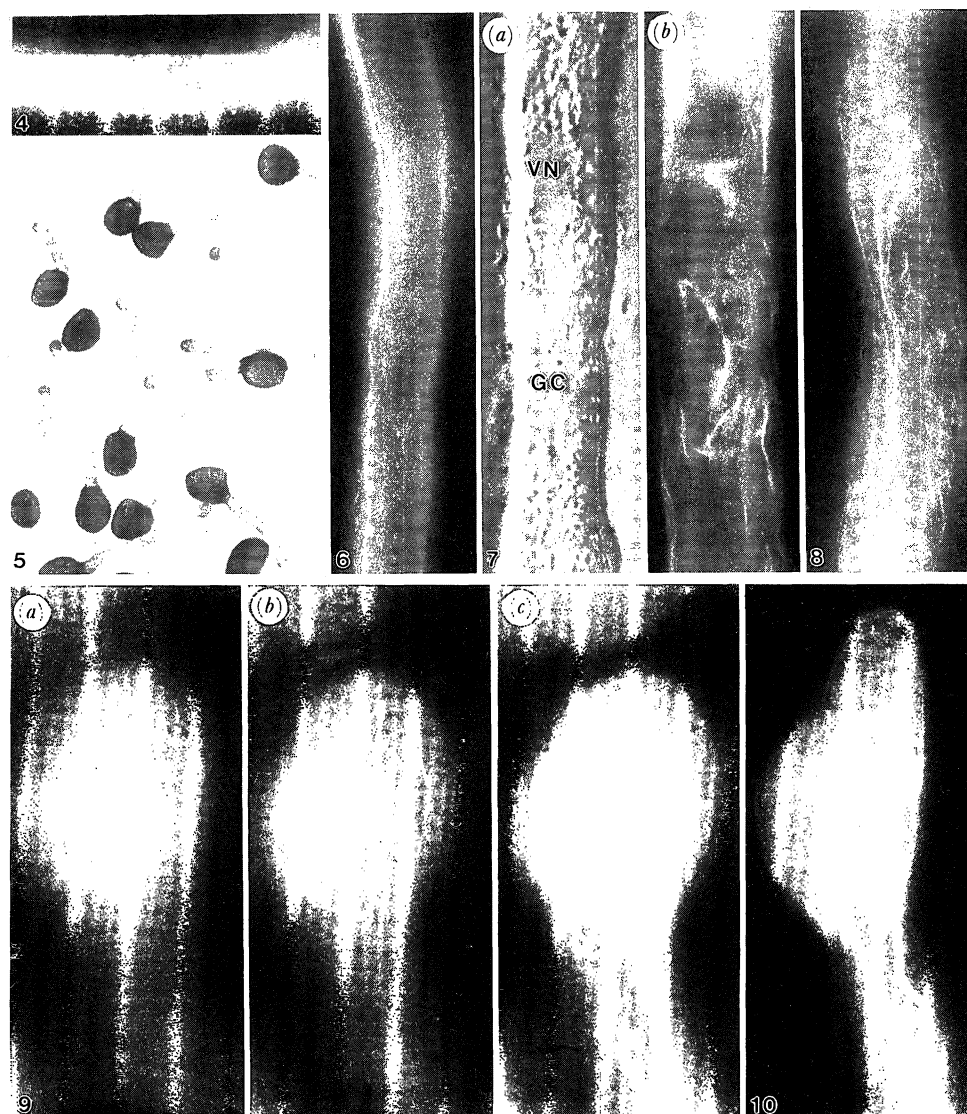
Figure 1. Control tube, showing the actin cytoskeleton in the sub-apical region. The arrow head shows the direction of the apex.

Figure 2. Sub-apical region, 70-min tube exposed to GM with $5 \mu\text{g ml}^{-1}$ CD for 15 min. Most of the fibrils have coalesced to form thicker cables, but occasional unfused stretches of the original slender fibrils remain.

Figure 3. Tube from the same culture as figure 2, segment in the vicinity of the vegetative nucleus, which is disposed to the right of the field, showing complex coiling of the thickened actin cables.

medium, clumping of the cytoplasm following during the subsequent 120 s, in a manner comparable with that described previously from *Iris* pollen tubes exposed to cytochalasin B (Heslop-Harrison & Heslop-Harrison 1989*a*). After 10 min in the CD medium the distal stretches of the arrested tubes of *E. nonscriptus* showed abnormal pectic wall thickenings, with some tubes already beginning to form terminal bulbs (figure 5). During this period of treatment most of the actin fibrils in the proximal parts of the tubes condensed to form thicker longitudinally oriented cables, usually few in number (figure 6). In the vicinities of the vegetative nucleus and generative cell the cables were commonly distorted, often appearing to remain wrapped around the surfaces of these larger inclusions of the vegetative cell (figures 7*a, b*).

During the first 10 min of recovery after return to normal GM, the actin cables progressively dissociated into individual fibrils in the proximal stretches of



Figures 4–10. Pollen tubes of *Endymion nonscriptus* grown for an initial period of 45 min in GM. Figure 4. Proximal region of a control tube at 45 min, Tr–Ph staining. (Magn. \times ca. 811.) Figure 5. Tubes exposed to GM with $5 \mu\text{g ml}^{-1}$ CD for 10 min, some showing first evidence of apical swelling. Alcian blue staining to reveal pectin accumulation at the tips. (Magn. \times ca. 130.) Figure 6. Sub-apical stretch of a tube similar to those of figure 5, Tr–Ph staining. (Magn. \times ca. 773.) Figure 7. (a) Tube from the culture of figure 5, segment containing the vegetative nucleus (VN) and the generative cell (GC). DIC micrograph. (b) Comparable field, Tr–Ph staining. (Magn. \times ca. 1080.) Figure 8. Sub-apical stretch of a tube after ca. 10 min recovery from CD treatment, showing restitution of the actin fibril system, Tr–Ph staining. (Magn. \times ca. 1040.) Figure 9. Through-focus sequence of the swollen apex of a tube comparable with that of figure 8, Tr–Ph staining. (a) Section plane near the proximal surface. (b) Section plane about $6 \mu\text{m}$ lower. (c) Section plane transecting the centre of the swelling and the axis of the parent tube. (Magn. \times ca. 1040.) Figure 10. Apical swelling of a tube from the same culture as that of figure 9, apparently showing the early initiation of a secondary tube tip. Tr–Ph staining. (Magn. \times ca. 1040.)

Figures 11–17. DIC micrographs of the apical zones of living pollen tubes of *Endymion nonscriptus* recovering in GM following 10 min in medium containing $5 \mu\text{g ml}^{-1}$ CD. All exposure times are approximate. (Magn. \times ca. 1050.)

viable tubes (figure 8). At the end of the 10-min period most tubes had developed conspicuous terminal swellings. No regular pattern of actin fibrils could be distinguished in these with the present methods of labelling. In the bulb shown in the through-focus micrograph sequence of figures 9a–c, extended fibrils were present in the older tube, some entering the swelling to pursue irregular paths near the wall. The micrograph of figure 9b appears to reveal shorter fibrils deeper in the cytoplasm, but the central zone, transected in figure 9c, shows mainly generalized

fluorescence. This was characteristic of most tubes surviving the preparation procedures in what was judged to be an essentially undamaged state. In no instances were local concentrations of shorter fibrils observed in the peripheral cytoplasm where they might be interpreted as marking the sites of prospective tube apices, even where the conformation of the wall suggested that a tube tip was already being defined (figure 10).

Continuous video recording and streak photography of living tubes revealed considerable diversity during

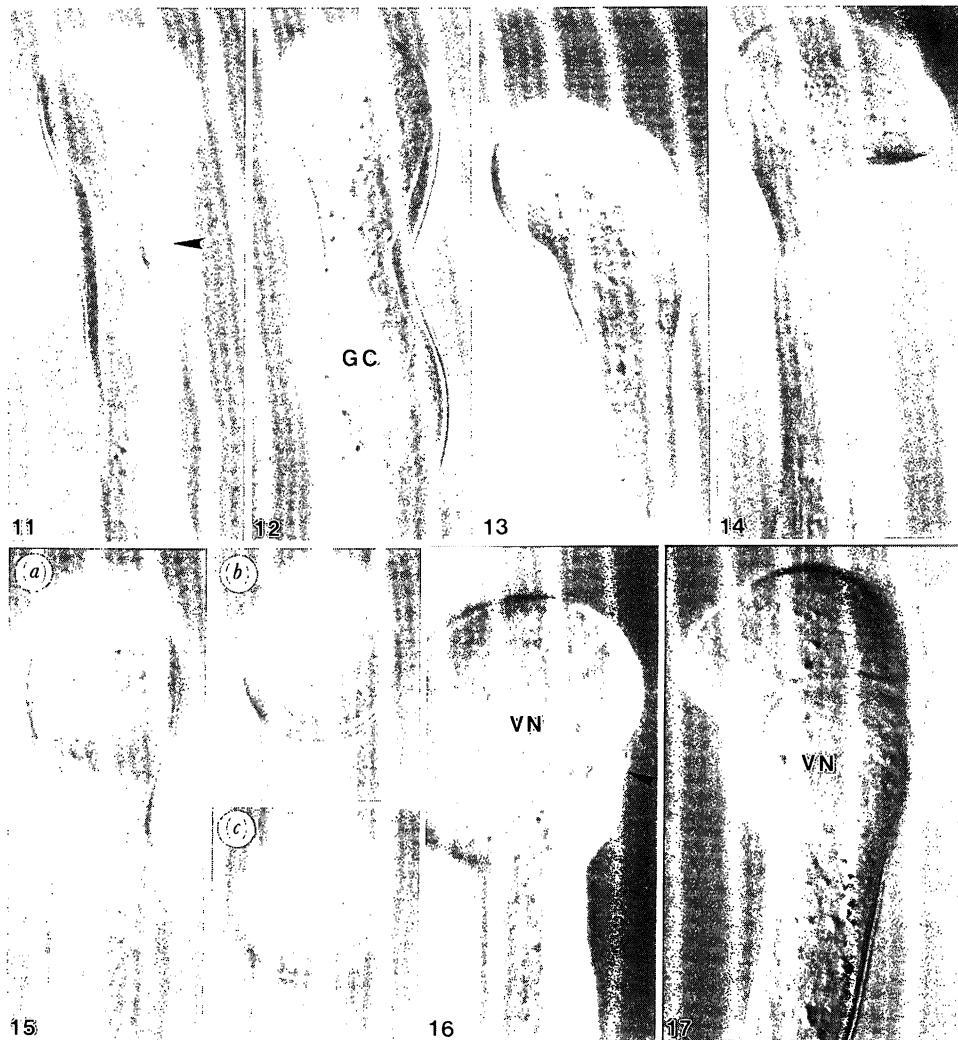
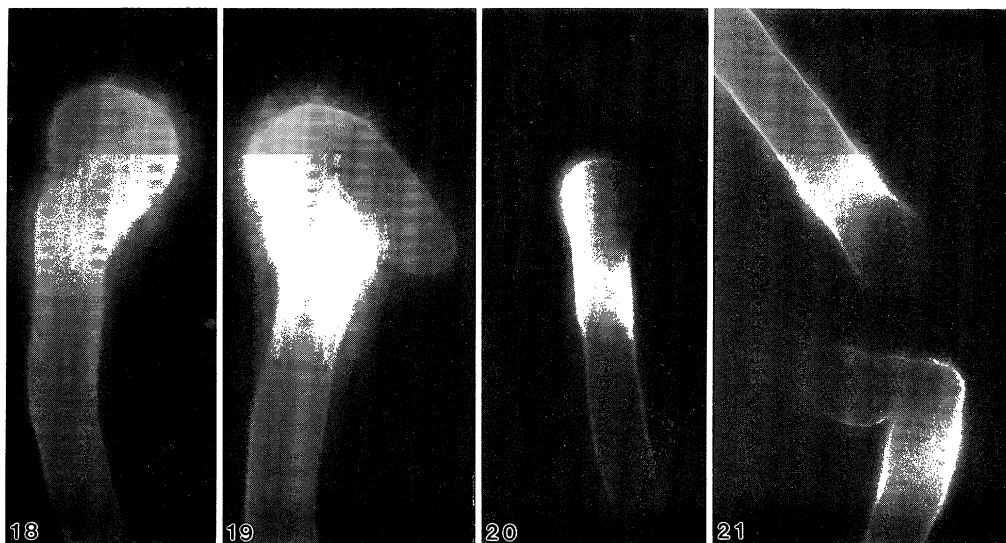


Figure 11. Swollen apex after 10 min recovery showing continuous wall thickening with occasional more massive wall swellings (arrow head). Such thickenings are irregularly multilamellate and chemically heterogeneous (Heslop-Harrison *et al.* 1990*b*). Exposure 6 s. Figure 12. As figure 11. Movement was sluggish in this tube, and the generative cell (GC), in which chromosomes can be distinguished, had moved towards the apex. Exposure 3 s. Figure 13. As figure 11. The flow pathways in this tube, which was swollen asymmetrically, entered the apex, and in the focal plane of this micrograph appeared to encircle a central core containing a stranded group of lipid globuli and organelles. Exposure 6 s. Figure 14. Tube after 15 min recovery with an emergence possibly defining a prospective secondary apex. While the flow pathways were well defined in the tube and into the apical swelling, movement in the emergence was random. As in the tube of figure 13, particulate inclusions in the centre of the apical bulb were static during the period of the exposure. Exposure 6 s. Figure 15. Tube comparable with that of Fig. 14, viewed in a sequence of 3 planes along the axis of the prospective apex. All exposures 6–8 s. (a) Focal plane transecting the parent tube. The flow pathways are well defined, and in this focal plane seem to continue around the apical swelling. The static bodies in the centre include both lipid globuli, distinguishable by higher refractive index, and rod-shaped mitochondria. (b) Focal plane near the base of the prospective tip. Most of the inclusions at this level are identifiable as mitochondria. (c) Focal plane near the extreme tip, showing mitochondria and smaller unidentifiable inclusions. Figure 16. Swollen, thin-walled prominence produced by a tube during a recovery period of 20 min. The outgrowth appears to have formed following the disruption of the original wall, remains of which can be seen to the right (arrow head). The vegetative nucleus (VN) has moved into the new outgrowth. Exposure 3 s. Figure 17. Tube from the same sample as that of figure 16. The outgrowth in this case is completely surrounded by a collar of material derived from the original wall of the terminal bulb, in which the vegetative nucleus (VN) can be distinguished. The emergence is forming a new tube apex, with the first evidence of organelle zonation. Exposure 3 s.

the recovery period, both in the pathways of movement of cytoplasmic inclusions and in the manner in which new adventitious tube tips were initiated. In a sample of 100 tubes, 20 showed no inclination to resume apical growth, even although movement was restored in the cytoplasm during recovery. Mostly this behaviour was associated with unbroken thickening of the wall over

the whole surface of the terminal bulb and along the length of the tube into the grain itself (figures 11–13). While normal movement pathways were re-established in the older parts of such blocked tubes, the ‘inverse fountain’ pattern of circulation characteristic of the original tube apex, with acropetal movement limited mainly to the periphery of the vegetative cell and



Figures 18 and 19. Apical zones of pollen tubes of *Endymion nonscriptus* during recovery from 10 min exposure to medium containing $5 \mu\text{g ml}^{-1}$ CD. CFW staining for cellulosic glucans. (Magn. \times ca. 830.) Figure 18. Initiation of a secondary apex; 10 min recovery period. Figure 19. Emergent secondary tube after the transition to cylindrical growth; 15–20 min recovery period.

Figures 20 and 21. As for figures 18 and 19, DAB staining for callose. Figure 20. Tube after a 10-min recovery period with a thin-walled emergence, likely to mark the site of a prospective apex, to the right of the apical swelling. (Magn. \times ca. 680.) Figure 21. Tubes from the same culture as that of figure 19. The upper of the pair has developed a secondary apex along the same axis as that of the parent tube, and is in the early stages of the transition to cylindrical growth, with a well-defined callosic sheath. The lower shows the more usual configuration, with the secondary tube, now in the cylindrical growth phase, having departed at an angle from the site of arrest. (Magn \times ca. 794.)

basipetal to a central core (figure 2 in Heslop-Harrison *et al.* (1990a)), was not restored at the tip. Organelles and other cytoplasmic inclusions entering this zone either moved randomly before joining a basipetal traffic stream, or followed complex trajectories around the tip before retreating irregularly along the tube.

From 10 min recovery onward the sites of prospective tube apices were progressively defined, albeit through a variety of processes. In some instances the locus of the new apex coincided with a zone of the wall where cellulosic and callosic thickening was less well developed (figures 18 and 21); in these sites the emerging tip was found to be thinly ensheathed in a pectic wall with a diffuse cellulosic component, differing little from that of the growing point of the normal tube. Although no consistent pattern of circulation could be distinguished in prospective tips like that of figure 14, the beginning of organelle zonation could occasionally be distinguished. This is revealed in the sequence of figure 15, in which a tip emerging from a living tube is seen in 'face' view. The focal plane of figure 15a intersects the parent tube near the base of the new outgrowth. Linear movement pathways can be discerned in the tube itself, and an irregular rotatory movement could also be seen around the periphery of the developing prominence. Lipid globuli and mitochondria in the central region were evidently moving less vigorously during the 6 s period of the exposure. In the higher focal plane of figure 15b, several essentially static mitochondria can be resolved. figure 15c, at a still higher level immediately within the tip, shows numerous small particulate bodies as well as occasional identifiable mitochondria. These expressed

mainly Brownian movement, and only occasionally were there indications of sustained passage from the periphery towards the centre such as might be expected were the movement in the tip to be of the inverse-fountain type.

An alternative mode of recovery involved the erosion and penetration of an already thickened wall to establish the prominence destined to form the new tube tip. The example shown in figure 16 shows a flap of detached wall material on the right of the tube, with a swollen thin-walled prominence overtopping it. Movement within this tube was sluggish during the period of observation, and it is open to question whether the early events in such an apex would indeed have been followed by the definition of a new growth centre. In contrast there is little ambiguity in interpreting the course of events associated with the aspect seen in the tube of figure 17. The micrograph shows a complete collar of material, apparently displaced from the original bulb wall, surrounding a thin-walled outgrowth, from which a tube tip of essentially normal aspect is emerging to the left. The zonation of organelles in the adventitious tip matches that to be expected in an actively extending tube, and the pattern of circulation during the period of observation was quite comparable with that of a normal apex.

Once a new apex was defined, cylindrical growth was rapidly assumed, and in samples taken from cultures at 15–20 min after transfer from the CD medium most viable tubes had terminal segments of virtually normal aspect. The mean diameter of the secondary tubes, $13.19 \pm 0.341 \mu\text{m}$ was greater than that of parent tubes, $11.90 \pm 0.349 \mu\text{m}$, but not

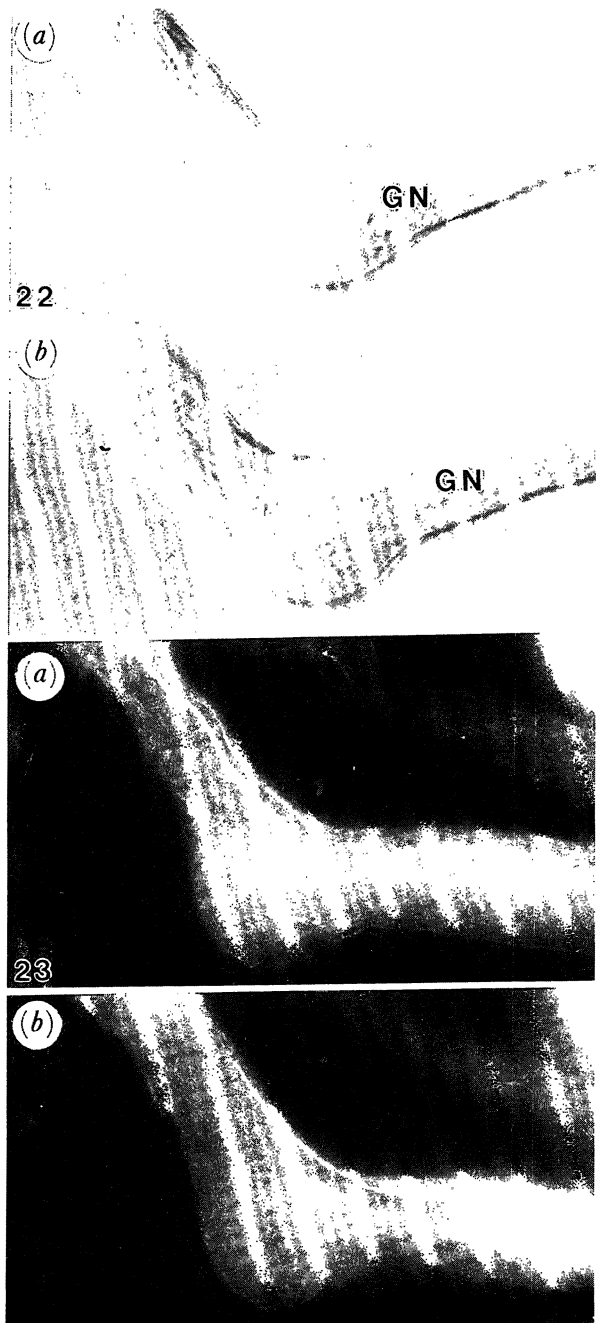


Figure 22. DIC micrographs of living pollen tubes of *Endymion non-scriptus*; 20 min recovery following 10 min in medium containing $5 \mu\text{g ml}^{-1}$ CD. (Magn. $\times ca.$ 1085.) The segment illustrated includes the swelling marking the site of arrest. The secondary tube has emerged and was extending actively at the time of the 3 s exposures. The principal flow pathways in the focal plane of the micrographs can be distinguished in both parent (left) and secondary (right) tubes, and also the tendency for moving bodies to follow the inner side of the bend, by-passing the residual swelling. (a) Generative cell (GN), identifiable by the chromosomes, at the site of the bend. (b) Same field *ca.* 4 min later, with the generative cell now moving through the secondary tube.

Figures 23(a) and (b). Segment of a tube comparable with that of figure 22 viewed in two focal planes. Tr-Ph staining; (magn. $\times ca.$ 1085.) The actin fibrils extend around the inside of the bend, defining the principal pathways of movement between the older (left) and newer (right) parts of the tube (*cf.* figure 22); none extends continuously through the residual swelling.

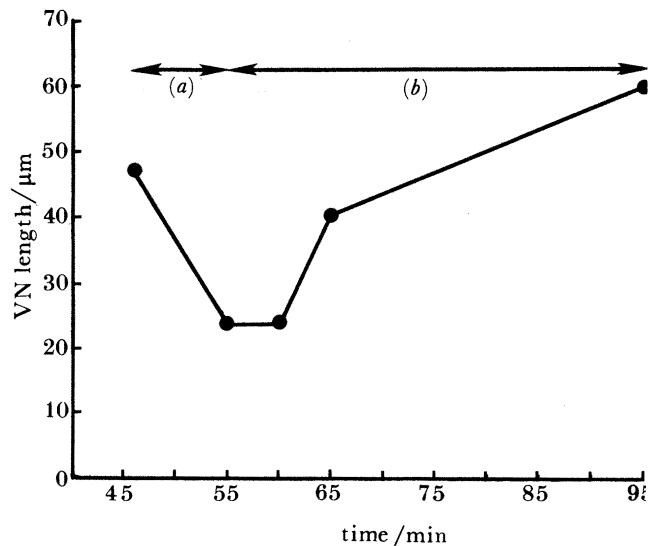


Figure 24. Overall lengths of vegetative nuclei in pollen tubes of *Endymion non-scriptus* responding to CD treatment (a) and during subsequent recovery (b).

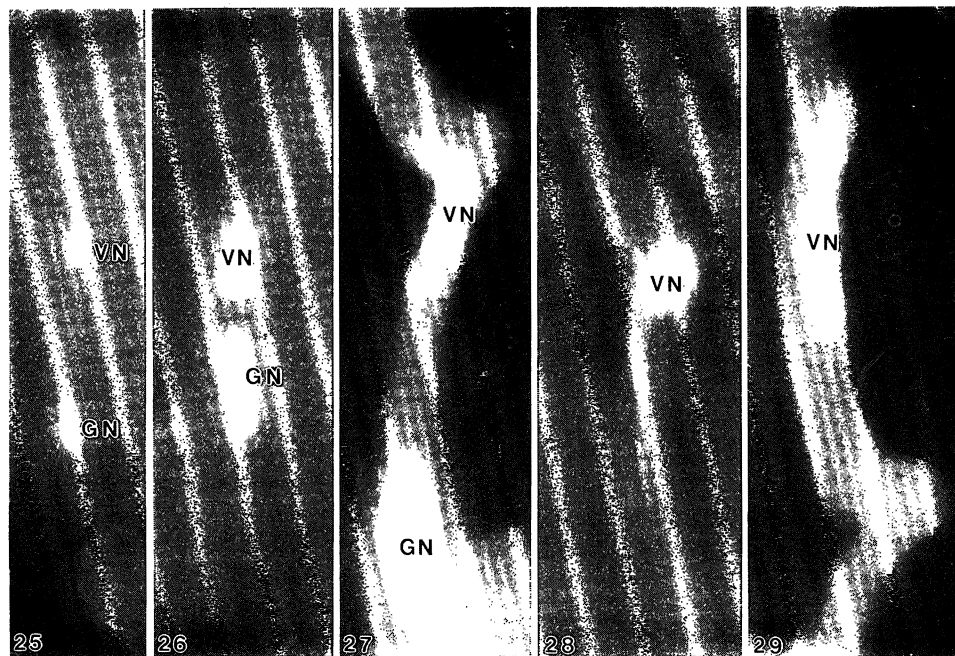
significantly so. The legacy of the period of suspended extension growth remained in distortions of the tube at the site of the original terminal bulb, and also in stretches of abnormal wall with mixed cellulose (figures 18 and 19) and callosic (figures 20 and 21) thickenings. After 60 min of recovery the mean length of the new segments of the tubes distal to the site of arrest was $338.5 \pm 31.65 \mu\text{m}$ ($n = 50$), implying a mean growth rate of some $0.094 \mu\text{m s}^{-1}$, virtually the same as that achieved in the final 20 min of growth before the beginning of treatment, estimated at $0.098 \mu\text{m s}^{-1}$.

Figures 22a and b, streak micrographs taken with an interval of about 4 min, reveal the disposition of traffic lanes linking the old and new segments of a tube after a recovery time of 20 min. The most rapid movement in the focal plane of these two micrographs was in the lanes on the inner side of the bend. In figure 22a the generative cell is seen to be held in the swollen part of the tube; in figure 22b it has escaped from this temporary arrest and is moving acropetally in the new segment.

Tr-Ph labelling of the actin in a segment of a tube like that of figure 22 shows that extended fibrils mainly follow the inner side of the bend (figures 23a, b), a disposition clearly correlated with the preferred pathways of organelle movement defined in figure 22. The presence of thicker cables in the stretch of the parent tube to the left in figure 23a suggests that in this case they were not wholly dissociated during the recovery period (*cf.* figure 8). In contrast, the fibril system in the new tube (figure 23b, right) is comparable with that in the parent tube before CD treatment (*cf.* figure 4).

(c) Behaviour of the vegetative nucleus

The mean length of the vegetative nuclei in actively elongating 45 min control tubes was $49.7 \pm 0.95 \mu\text{m}$ ($n = 25$). During a 10 min period of CD treatment the nuclei contracted along the length of the tubes to $23.4 \pm 1.08 \mu\text{m}$ ($n = 25$), extending again as movement



Figures 25–29. Pollen tubes of *Endymion nonscriptus* following 10 min in medium containing $5 \mu\text{g ml}^{-1}$ CD. DAPI staining for the nuclei of the vegetative (VN) and generative cells (GN). The tube tip is to the top of each micrograph. Figure 25 (Magn. $\times ca.$ 229); remainder magn. $\times ca.$ 615.) Figure 25. Disposition of VN and GN in a pollen tube from a culture comparable with that of figure 5, immediately following CD treatment. The VN is condensed along the length of the tube, and in this instance the VN leads the GN by $70 \mu\text{m}$. There are no persistent links between the vegetative and generative cells in this species. Figure 26. As figure 25, earlier stage of emergence of the generative cell and VN. The residual prominences on the latter mark the likely sites of former links to actin fibrils. Figure 27. Tube 20 min into recovery, VN entering the site of arrest and beginning to by-pass the CD-induced swelling. In this instance the diameter of the secondary tube was substantially greater than that of the original. Figure 28. As figure 27; VN delayed in the CD-induced swelling. Long pointed processes extend in both directions along the tube, indicating association with differently polarized elements of the actin cytoskeleton (Heslop-Harrison and Heslop-Harrison 1989*b*) and illustrating the great elasticity of the nuclear envelop. Figure 29. VN progressing through the secondary tube. The extended state is that to be expected in normal tubes of this age.

in the cytoplasm was resumed after restoration to normal GM (figure 24), to reach a length of $60.5 \pm 3.17 \mu\text{m}$ ($n = 25$) at 40 min, when the age of the tubes was 95 min. Characteristic conformations of the condensed and immobilized nuclei in the original tube immediately after exposure to CD are shown in figures 25 and 26. Figure 27, of a tube 20 min into recovery, shows the vegetative nucleus negotiating the site of the CD-induced arrest to enter the secondary tube, with the generative cell just leaving the grain. Occasionally the nucleus was delayed in the swelling, and in the example seen in figure 28, slender, pointed processes extend in both directions along the tube, indicating that opposed forces have been applied to its surface, presumably in consequence of local associations with differently polarized actin fibrils near the inner side of the bend where the continuous fibril system is concentrated (figure 23). The vegetative nucleus in figure 29 has left the site of the initial arrest, and shows the elongated aspect customarily found in actively extending normal tubes.

In the normal tube the vegetative nucleus tends to track the apex, maintaining a roughly constant distance from it during the course of growth. In 45-min control tubes the mean distance from the leading edge of the vegetative nucleus to the tube tip was

$139.5 \pm 5.45 \mu\text{m}$ ($n = 25$). After a 60-min recovery period the mean distance from the apex in tubes cultured for 10 min in the CD medium was $142.9 \pm 14.36 \mu\text{m}$ ($n = 25$), not significantly different from the separation preceding treatment. However, the nuclei were dispersed more widely along the treated tubes, with a range of 57.0 – $357.2 \mu\text{m}$, compared with a range of 91.2 – $197.6 \mu\text{m}$ in controls. This undoubtedly reflects the erratic movement of the vegetative nuclei during and following treatment, notably their varying efficiency in negotiating distortions in the tube at the sites of arrest.

4. DISCUSSION

The present observations on the pollen tubes of *N. pseudonarcissus* add weight to the conclusion of Lancelle & Hepler (1988) that one conspicuous effect of the cytochalasins is to cause the microfilaments of the vegetative cell to aggregate in massive, randomly oriented bundles. The method of Tr-Ph labelling used in the present study conserves finer elements of the actin cytoskeleton in the normal tubes of *N. pseudonarcissus* (figure 1), suggesting that some reliance may be placed on the results obtained from CD-treated tubes prepared in an identical manner. Elements of the

system evidently condense into thicker cables in response to treatment, leaving occasional slender fibrils partly adherent to the larger aggregates (figure 2). Such images would seem to support the further conclusion of Lancelle & Hepler (1988) that the massive bundles are produced by coalescence and not by disaggregation of the finer fibrils followed by repolymerization.

These results can be reconciled in part with earlier observations on the effect of CD on the extended fibrils of the pollen tubes of *Iris* which provide the pathways for long-range passage of organelles. Because these lie separately in the older parts of the vegetative cell, their fate during CD treatment can readily be followed and recorded in the living state. A frequent response to the treatment is the gradual apposition of individual fibrils to form thicker strands, which may remain suspended in the tube centre, or collapse towards the adjacent wall (Heslop-Harrison & Heslop-Harrison 1989*a*). Such behaviour accords well enough with the proposition that the cytochalasin treatment in this instance brings about aggregation of lesser filament bundles into more massive cables. However, direct observation of events in living tubes showed that the original fibrils do occasionally fragment and retract in response to treatment. We have also observed fragmentation of parts of the actin fibril system of the pollen tubes of *Galanthus nivalis* in response to CD (Heslop-Harrison & Heslop-Harrison 1989*b*), and while we now recognize that the preparation procedures for Tr-Ph labelling in their earlier study, which involved the use of EGTA in the permeabilizing medium, may have been less than adequate, we do not discount the main results. Radical structural changes in the cytoplasm occur during CD treatment, including the rapid redistribution of essentially all of the constituents of the vegetative cell (Heslop-Harrison *et al.* 1990*b*), and it is entirely probable that these could result in local shearing and segmentation of actin fibrils as a secondary, mechanical, effect. The safest conclusion at present seems to be that the cytochalasins may induce both aggregation and fragmentation of the actin fibril system in the complex environment of the pollen tube.

The speedy resumption of activity in the tubes upon return to GM after CD-induced paralysis implies that whatever the state of the actin fibrils at the end of treatment, a functional motility system is regenerated very rapidly in normal GM, at least in some domains of the vegetative cell. The micrograph of figure 8 suggests that in the segment of the tube present at the time of treatment this is achieved by the dissociation of fibril aggregates like that of figure 6 to produce a system of thin fibrils comparable with that of the normal tube, albeit rather less regular. Such a system of mainly longitudinally oriented fibrils extends up to the terminal swelling (figures 9 and 10), but in the swelling itself the paths are not well defined, and the impression is of dispersed shorter fibrils surrounding a central zone which reveals mainly generalized fluorescence following Tr-Ph labelling. The presence of well stained fibrils in the parent tubes argues against this aspect being artefactual.

A noteworthy feature of the development of new

adventitious tubes after CD-induced arrest was the establishment of movement pathways linking with those of the parent tube but by-passing much of the terminal swelling, especially where the new tube had departed at an angle. Continuous observation of living tubes showed that organelles were frequently stranded in the by-passed volume, and that both vegetative nuclei and generative cells could be delayed in their passage if they entered the by-passed part. The routes and disposition of the actin fibrils through the zone provide the clue to understanding this behaviour: the continuous fibrils, which appeared often to be thicker than those of the parent tube, tended to follow the inner track where the tube was bent, with few entering the swollen zone.

Figure 24 shows that the vegetative nucleus of the pollen tube of *E. nonscriptus* contracts to about half of its original length during a 10-min exposure to the CD medium, a response attributable to the release of opposed tensions on the nucleus surface following the corruption of the actin fibril system. During recovery in normal GM the nucleus elongates once more in step with the restitution of the normal fibril system (figure 8), a further indication that the shape changes result from interaction with the actin cytoskeleton. Both the vegetative nucleus and the generative cell may advance further towards the tube tip during the period of treatment and early recovery (figures 12, 16 and 17), but, predictably, sustained movement away from the grain is only resumed where a new adventitious tube emerges and extension growth is re-established.

This study, while elucidating details of some of the structural events associated with the restoration of pollen tube growth and movement within the vegetative cell following temporary CD paralysis, leaves unanswered the question of why blocked apices should produce prominences during recovery which rapidly adopt a cylindrical mode of growth instead of simply enlarging isodiametrically. It seems that there is no consistent mechanism for the initiation of new growing points, even amongst tubes treated with the greatest possible uniformity. Earlier studies of the comportment of the actin cytoskeleton during pollen germination (Heslop-Harrison *et al.* 1986; Tiwari & Polito 1988) may lead one to expect that the sites of prospective new tube apices during regeneration would be marked by convergent fibrils and local aggregates of shorter strands, but no evidence of this has as yet been obtained from *E. nonscriptus*. New growing points are recognizable, once defined, by investment in a thinner, mainly pectic wall, and in the living tube by the gradual establishment of cytoplasmic zonation, first apparent in the exclusion of larger organelles from the growth centre itself as seen in figure 14, 15 and 17. The thin-walled, initially hemispherical, outgrowths may develop directly from the terminal swellings, presumably through the stretching of local areas of weakness in the original wall under hydrostatic pressure, or in a more spectacular manner by bursting through the thickened wall, as in the tube of figure 17.

Significantly, both during pollen germination and in the formation of adventitious tubes from temporarily arrested apices, the transition from the hemispherical

state to cylindrical growth is associated with the earliest deposition of the inner callose sheath. This forms a girdle around the base of the emergent tube, and is thenceforth propagated acropetally in step with the advancing apex. The sheath presumably provides the radial constraint that prevents isodiametric expansion and ensures the maintenance of the cylindrical form, much in the manner of the circumferentially disposed cellulose microfibrils in other types of cylindrical, tip-growing plant cells. The mechanism that determines the sequential deposition of pectic, cellulosic and callosic wall constituents basipetally from the extreme tip could therefore be a key determinant. Control of wall stratification in the apical zone is undoubtedly related to the functioning of the motility system in the vegetative cell. The zonation in the cytoplasm of the tube is linked to a distinctive pattern of circulation of organelles and other constituents, and is intimately concerned with the vectorial transport of the polysaccharide-containing wall precursor bodies (Heslop-Harrison & Heslop-Harrison 1990*a*). When the motility system is paralysed by cytochalasin treatment, the apical zonation is lost, the polarized delivery of wall material is disrupted, and wall thickening becomes generalized, with no standard stratification (figures 11 and 12; Heslop-Harrison *et al.* 1990*b*).

While the analogy with the germination process is attractive, it may be inappropriate to press it too far. An alternative mode of initiating cylindrical growth is, in fact, already known, albeit one which does not seem to have a parallel in the regeneration of cytochalasin-blocked tubes. In a recent paper Rutten & Derksen (1990) have described the remarkable way in which tube-like outgrowths are initiated from subprotoplasts derived from pollen tubes of *Nicotiana tabacum*. In this instance, the site of outgrowth was often found to be demarcated by a peripheral ring of actin filaments, and in the outgrowing tube actin fibrils were seen to be oriented perpendicularly to the direction of growth.

Finally there remains the question of a possible role for the microtubule cytoskeleton during regeneration. We have examined aspects of this in a parallel study, and have found that the regeneration processes, including the initiation of new tube tips, the transition to cylindrical growth and the resumption of movement, are not inhibited by concentrations of colchicine that eliminate microtubules from the vegetative cell. We propose to report the results of the investigation in detail in a further paper, but it may be noted here that this finding seems to discount the possibility that microtubules play a key part in the morphogenetic events associated with the regeneration of the tube apex and the establishment of cylindrical growth.

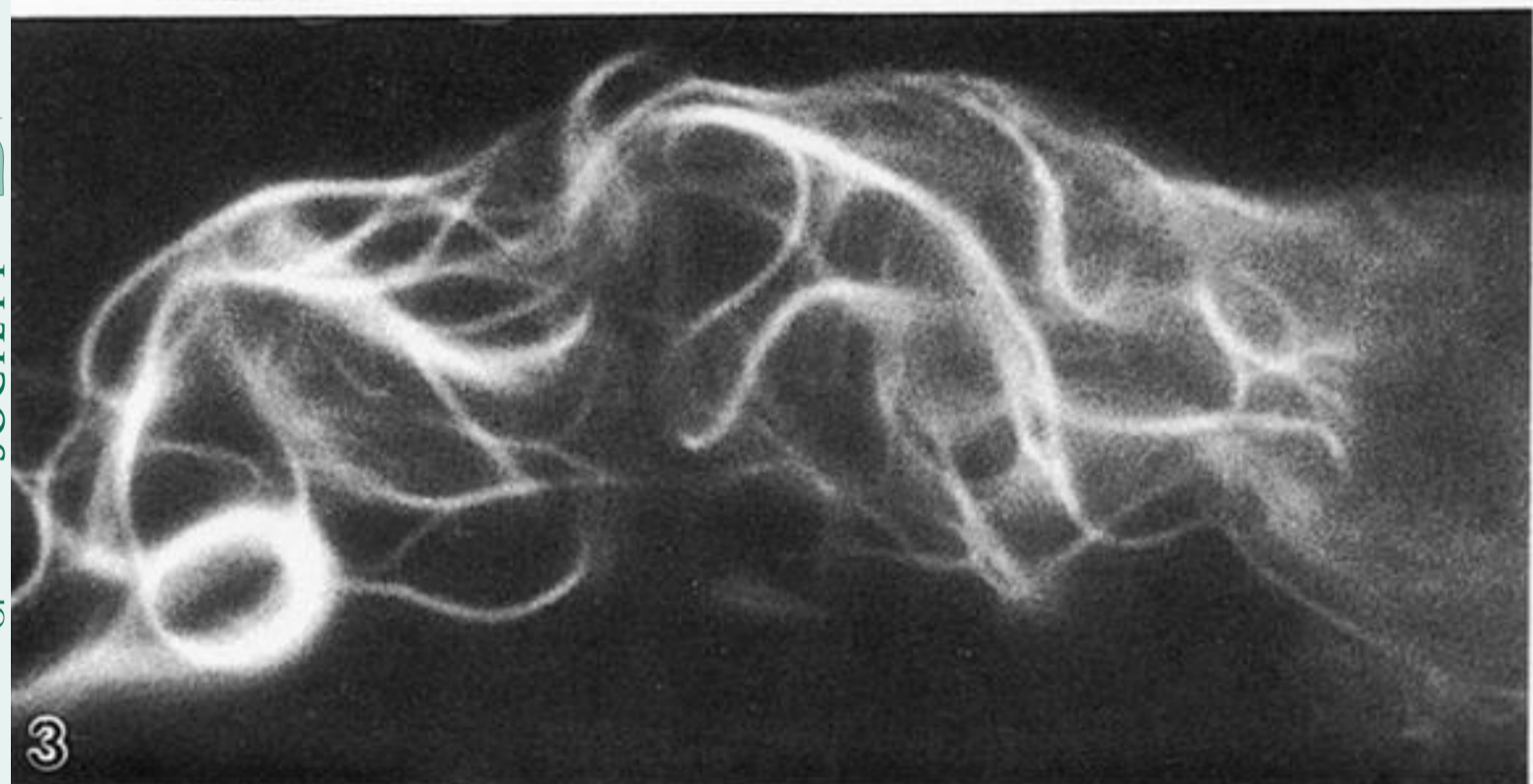
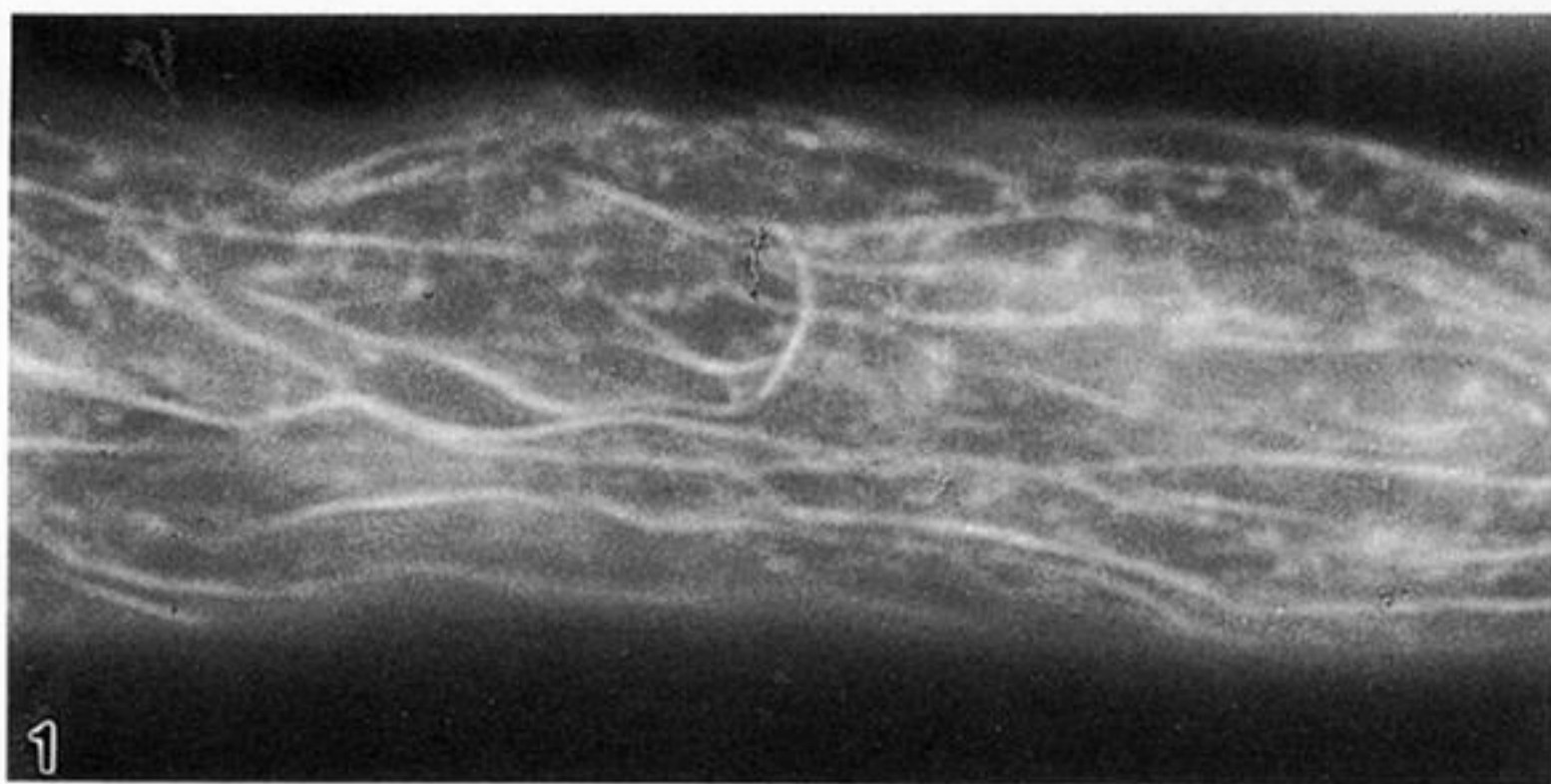
We are grateful to the Director of the Institute of Grassland and Ecological Research for facilities afforded us during this study, which was supported in part by a grant from the Agriculture and Food Research Council under the Cell Signalling and Recognition programme.

REFERENCES

- Bradley, M. O. 1973 Microfilaments and cytoplasmic streaming: inhibition of streaming with cytochalasin. *J. Cell Sci.* **12**, 327–343.
- Cooper, J. A. 1987 Effects of cytochalasin and phalloidin on actin. *J. Cell Biol.* **105**, 1472–1478.
- Cresti, M., Hepler, P. K., Tiezzi, A. & Ciampolini, F. 1986 Fibrillar structures in *Nicotiana* pollen tubes: changes in ultrastructure during pollen activation and tube emission. In *Biotechnology and ecology of pollen* (ed. D. L. Mulcahy, G. Mulcahy & E. Ottaviano), pp. 283–288. New York: Springer-Verlag.
- Forer, A., Emmersen, J. & Behnke, O. 1972 Cytochalasin B: does it affect actin-like filaments? *Science, Wash.* **175**, 774–775.
- Franke, W. W., Herth, W., Van der Woude, W. J. & Morré, D. J. 1972 Tubular and filamentous structures in pollen tubes: possible involvement as guide elements in protoplasmic streaming and vectorial migration of secretory vesicles. *Planta* **105**, 317–341.
- Heslop-Harrison, J. & Heslop-Harrison, Y. 1984 The disposition of gamete and vegetative cell nuclei in the extending pollen tubes of a grass species, *Alopecurus pratensis*. *Acta bot. neerl.* **33**, 131–134.
- Heslop-Harrison, J. & Heslop-Harrison, Y. 1985 Germination of stress-tolerant *Eucalyptus* pollen. *J. Cell Sci.* **73**, 135–137.
- Heslop-Harrison, J. & Heslop-Harrison, Y. 1987 An analysis of gamete and organelle movement in the pollen tube of *Secale cereale* L. *Plant Sci.* **51**, 203–213.
- Heslop-Harrison, J. & Heslop-Harrison, Y. 1988 Organelle movement and fibrillar elements of the cytoskeleton in the angiosperm pollen tube. *Sex. Plant Reprod.* **1**, 16–24.
- Heslop-Harrison, J. & Heslop-Harrison, Y. 1989*a* Cytochalasin effects on structure and movement in the pollen tube of *Iris*. *Sex. Plant Reprod.* **2**, 27–37.
- Heslop-Harrison, J. & Heslop-Harrison, Y. 1989*b* Conformation and movement of the vegetative nucleus of the angiosperm pollen tube: association with the actin cytoskeleton. *J. Cell Sci.* **93**, 299–308.
- Heslop-Harrison, J. & Heslop-Harrison, Y. 1990*a* Dynamic aspects of apical zonation in the angiosperm pollen tube. *Sex. Plant Reprod.* **3**, 187–194.
- Heslop-Harrison, J., Heslop-Harrison, Y., Cresti, M. & Ciampolini, F. 1990*b* Ultrastructural features of pollen tubes of *Endymion non-scriptus* modified by cytochalasin D. *Sex. Plant Reprod.* **4**. (In the press.)
- Heslop-Harrison, J., Heslop-Harrison, Y., Cresti, M., Tiezzi, A. & Ciampolini, F. 1986 Actin during pollen germination. *J. Cell Sci.* **86**, 1–8.
- Heslop-Harrison, J., Heslop-Harrison, Y., Cresti, M., Tiezzi, A. & Moscatelli, A. 1988 Cytoskeletal elements, cell shaping and movement in the angiosperm pollen tube. *J. Cell Sci.* **91**, 49–60.
- Lancelle, S. A., Cresti, M. & Hepler, P. K. 1987 Ultrastructure of the cytoskeleton in freeze-substituted pollen tubes of *Nicotiana glauca*. *Protoplasma* **140**, 141–150.
- Lancelle, S. A. & Hepler, P. K. 1988 Cytochalasin-induced structural alterations in *Nicotiana* pollen tubes. *Protoplasma* **2 (Suppl.)**, 65–75.
- Mascarenhas, J. P. & Lafountain, J. 1972 Protoplasmic streaming, cytochalasin B and the growth of the pollen tube. *Tissue Cell* **4**, 11–14.
- Miranda, A. F., Godman, G. C. & Tanenbaum, S. W. 1974 Action of cytochalasin D on cells of established lines. II Cortex and microfilaments. *J. Cell Biol.* **62**, 406–423.
- Pierson, E. S. 1988 Rhodamine-phalloidin staining of F-actin in pollen after dimethylsulphoxide permeabilisation.

- A comparison with the conventional formaldehyde preparation. *Sex. Plant Reprod.* **1**, 83–87.
- Rathke, P. C., Seib, E., Weber, K., Osborn, M. & Franke, W. W. 1977 Rod-like elements from actin-containing microfilament bundles observed in cultured cells after treatment with cytochalasin A (CA). *Expl Cell Res.* **105**, 253–262.
- Rutten, T. L. M. & Derksen, J. 1990 Organisation of actin filaments in regenerating and outgrowing subprotoplasts from pollen tubes of *Nicotiana tabacum* L. *Planta* **180**, 471–479.
- Schliwa, M. 1982 Action of cytochalasin D on cytoskeletal networks. *J. Cell Biol.* **92**, 79–91.
- Staiger, C. J. & Schliwa, M. 1987 Actin localisation and function in higher plants. *Protoplasma* **141**, 1–12.
- Tiwari, S. C. & Polito, V. S. 1988 Spatial and temporal organisation of actin during hydration, activation and germination of pollen of *Pyrus communis* L.: a population study. *Protoplasma* **147**, 5–15.
- Wessels, N. K., Spooner, B. S., Ash, J. F., Bradley, M. O., Luduena, M. A., Taylor, E. L., Wrenn, J. T. & Yamada, K. M. 1971 Microfilaments in cellular and developmental processes. *Science, Wash.* **171**, 335–343.
- Williamson, R. E. 1986 Organelle movements along actin filaments and microtubules. *Plant Physiol.* **82**, 631–634.

Received 3 October 1990; accepted 15 November 1990

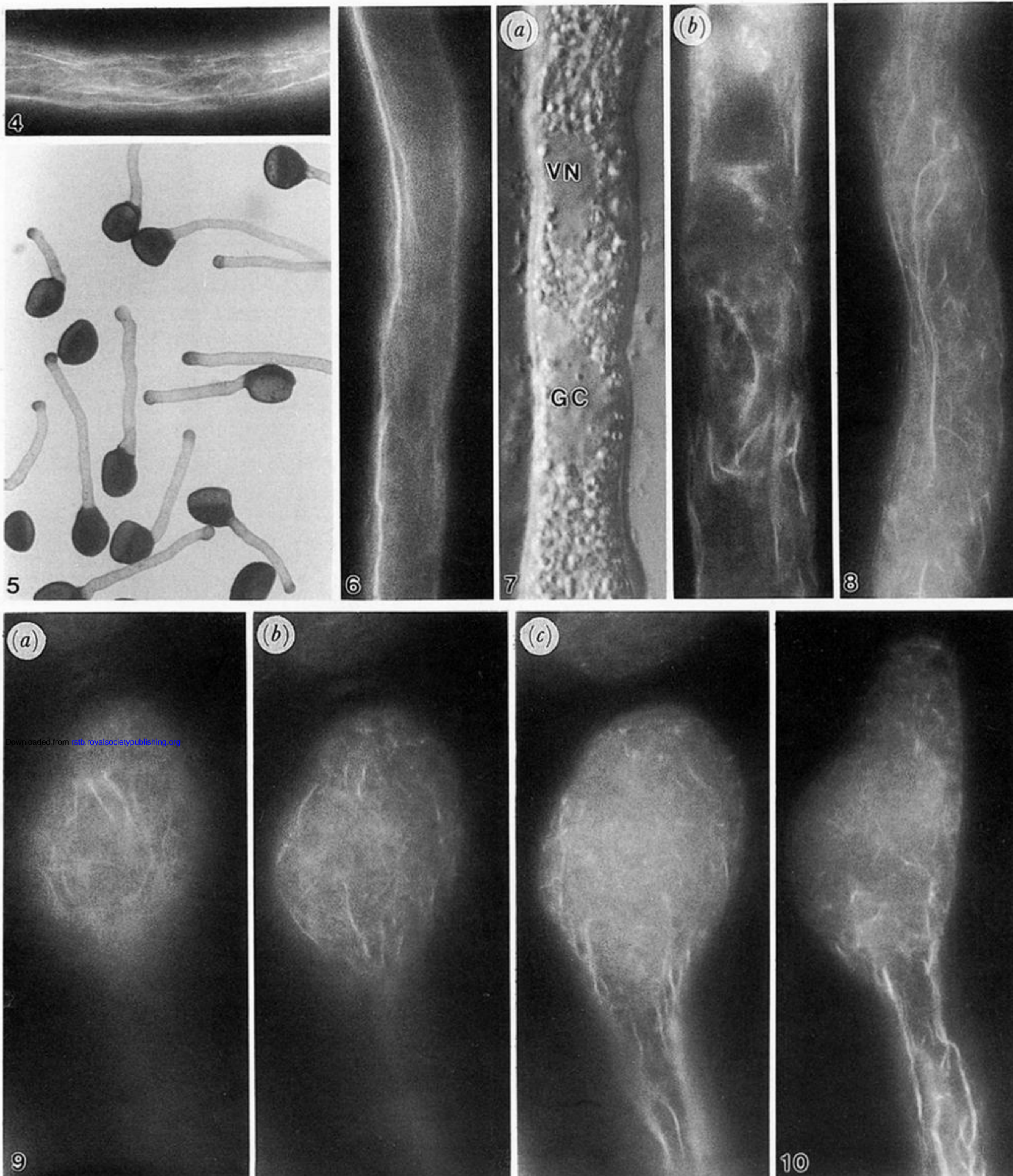


Figures 1–3. Unfixed pollen tubes of *Narcissus pseudonarcissus* (70 min from initial hydration in GM, Tr–Ph staining. Magn. $\times ca.$ 2173.)

Figure 1. Control tube, showing the actin cytoskeleton in the sub-apical region. The arrow head shows the direction of the apex.

Figure 2. Sub-apical region, 70-min tube exposed to GM with $5 \mu\text{g ml}^{-1}$ CD for 15 min. Most of the fibrils have coalesced to form thicker cables, but occasional unfused stretches of the original slender fibrils remain.

Figure 3. Tube from the same culture as figure 2, segment in the vicinity of the vegetative nucleus, which is disposed to the right of the field, showing complex coilings of the thickened actin cables.



Figures 4–10. Pollen tubes of *Endymion nonscriptus* grown for an initial period of 45 min in GM. Figure 4. Proximal region of a control tube at 45 min, Tr–Ph staining. (Magn. $\times ca.$ 811.) Figure 5. Tubes exposed to GM with $5 \mu\text{g ml}^{-1}$ CD for 10 min, some showing first evidence of apical swelling. Alcian blue staining to reveal pectin accumulation at the tips. (Magn. $\times ca.$ 130.) Figure 6. Sub-apical stretch of a tube similar to those of figure 5, Tr–Ph staining. (Magn. $\times ca.$ 773.) Figure 7. (a) Tube from the culture of figure 5, segment containing the vegetative nucleus (VN) and the generative cell (GC). DIC micrograph. (b) Comparable field, Tr–Ph staining. (Magn. $\times ca.$ 1080.) Figure 8. Sub-apical stretch of a tube after *ca.* 10 min recovery from CD treatment, showing restitution of the actin fibril system, Tr–Ph staining. (Magn. $\times ca.$ 1040.) Figure 9. Through-focus sequence of the swollen apex of a tube comparable with that of figure 8, Tr–Ph staining. (a) Section plane near the proximal surface. (b) Section plane about $6 \mu\text{m}$ lower. (c) Section plane transecting the centre of the swelling and the axis of the parent tube. (Magn. $\times ca.$ 1040.) Figure 10. Apical swelling of a tube from the same culture as that of figure 9, apparently showing the early initiation of a secondary tube tip. Tr–Ph staining. (Magn. $\times ca.$ 1040.)

Figures 11–17. DIC micrographs of the apical zones of living pollen tubes of *Endymion nonscriptus* recovering in GM following 10 min in medium containing $5 \mu\text{g ml}^{-1}$ CD. All exposure times are approximate. (Magn. $\times ca.$ 1050.)

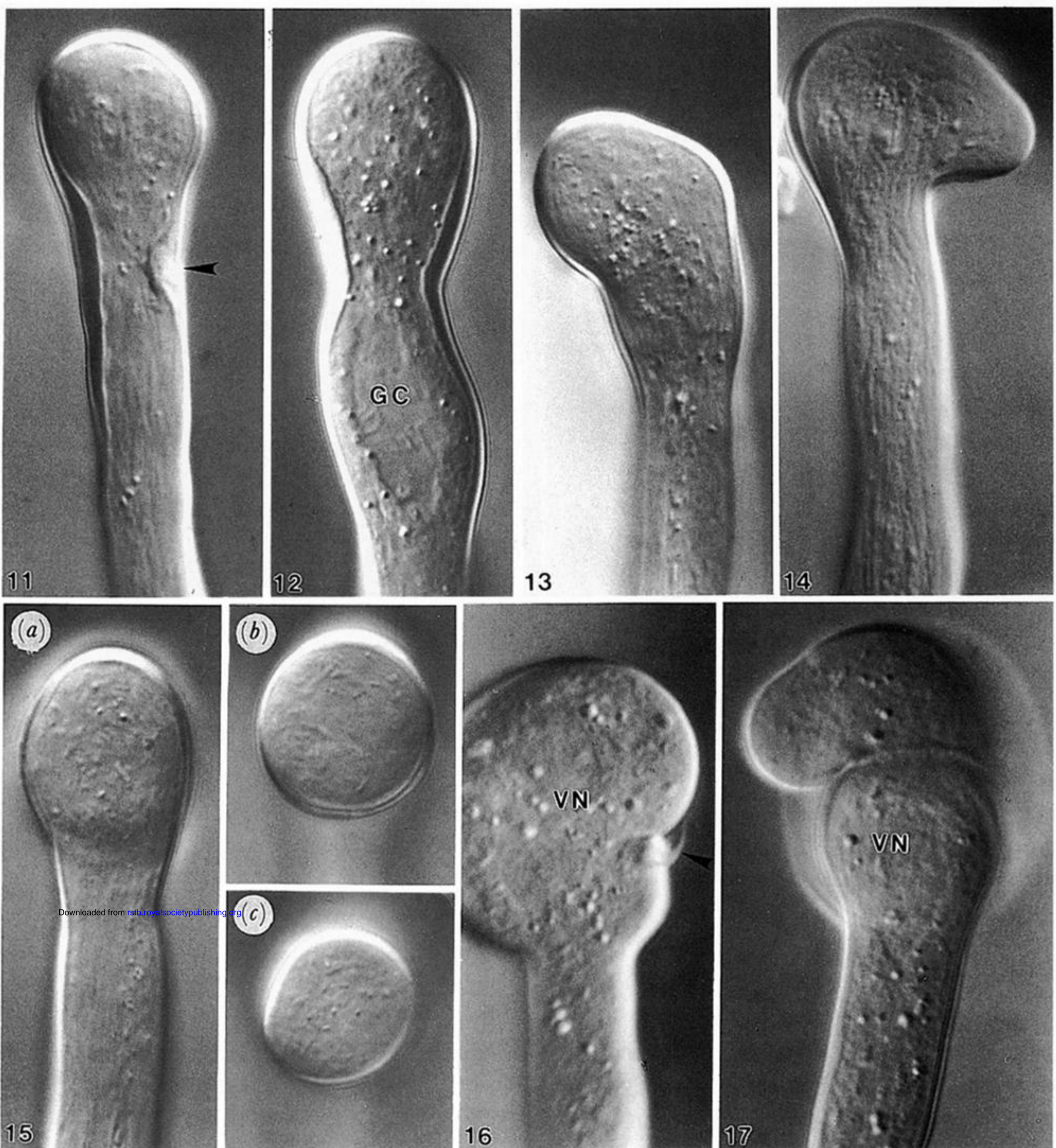
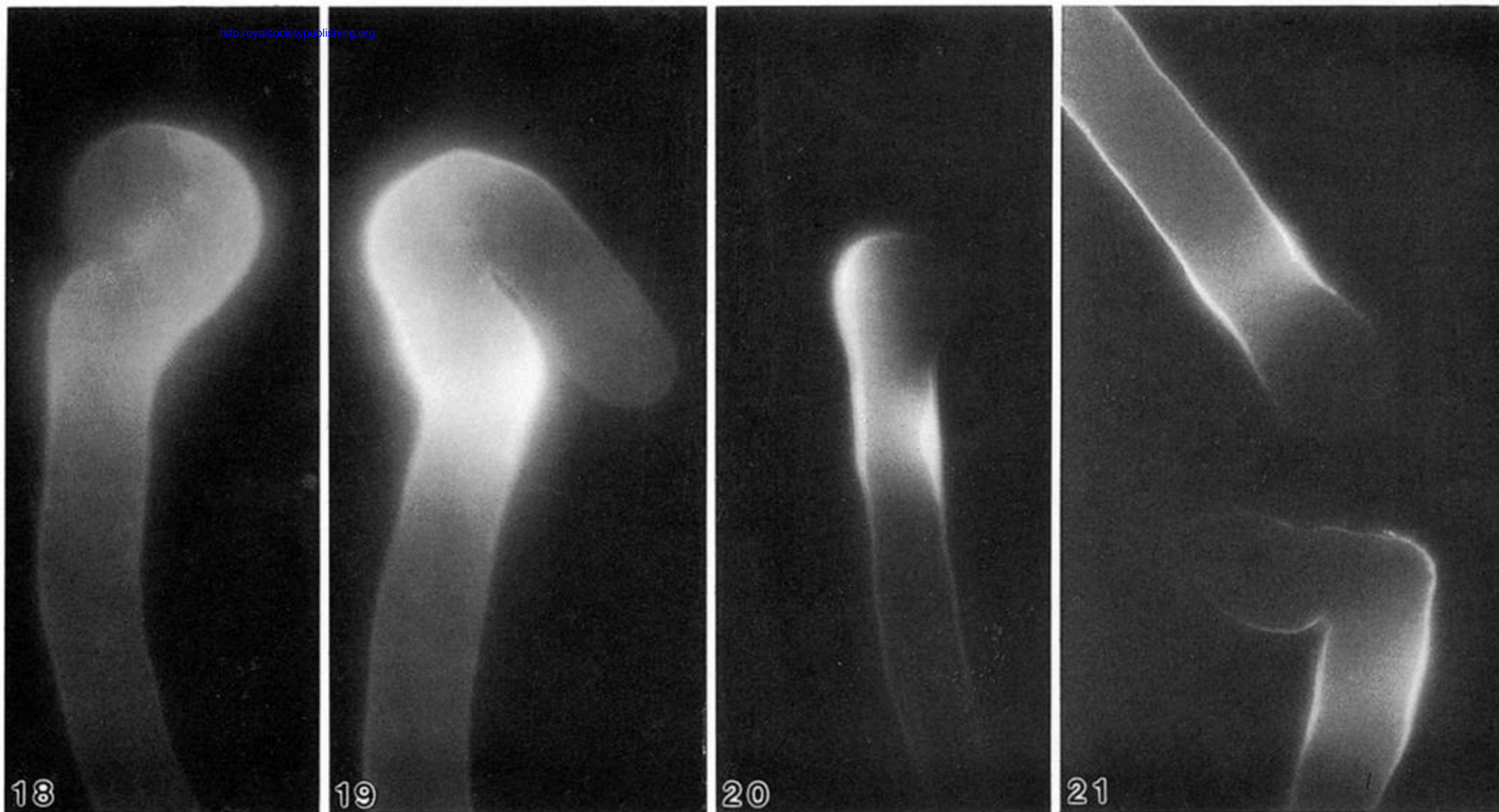
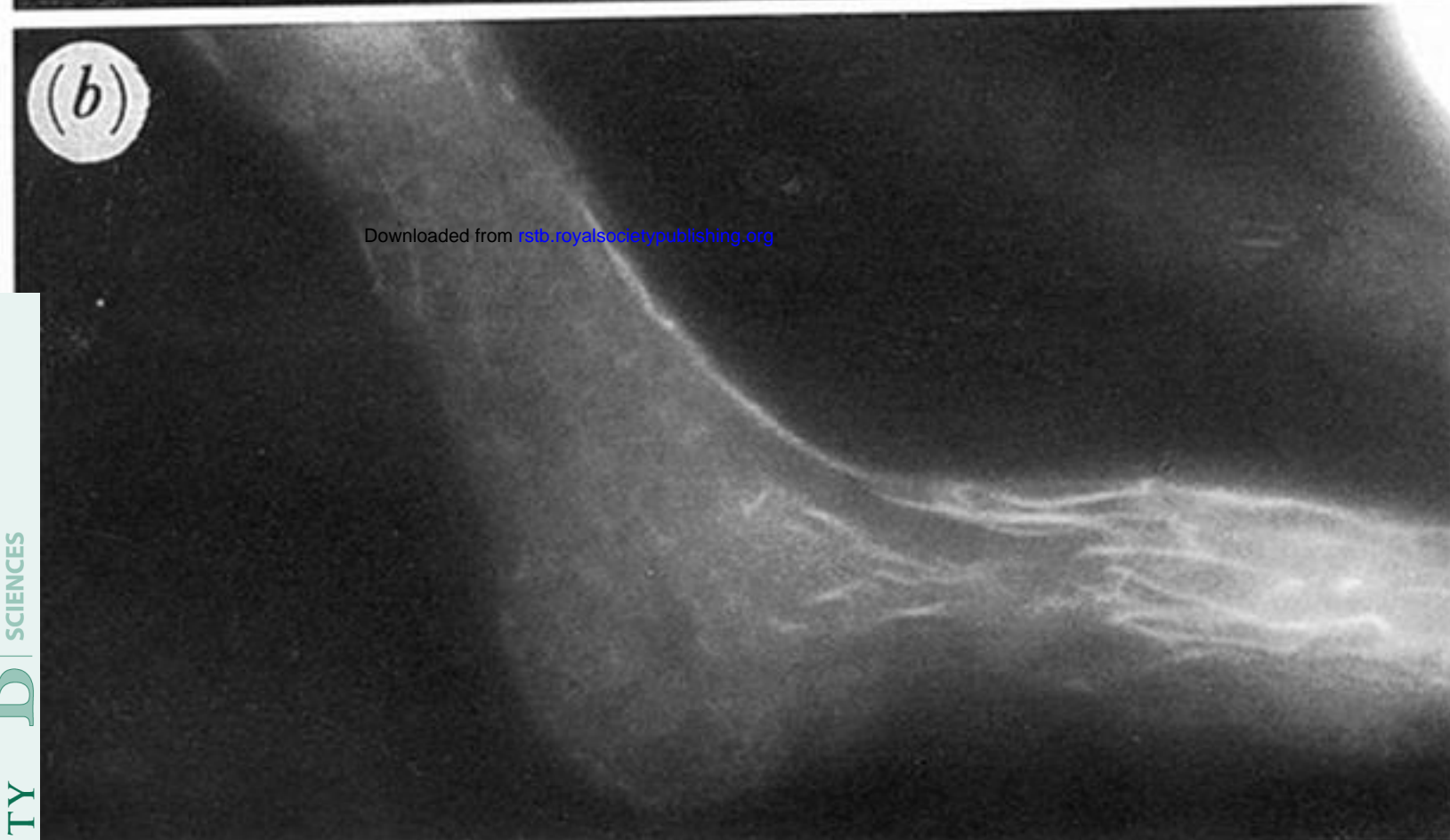
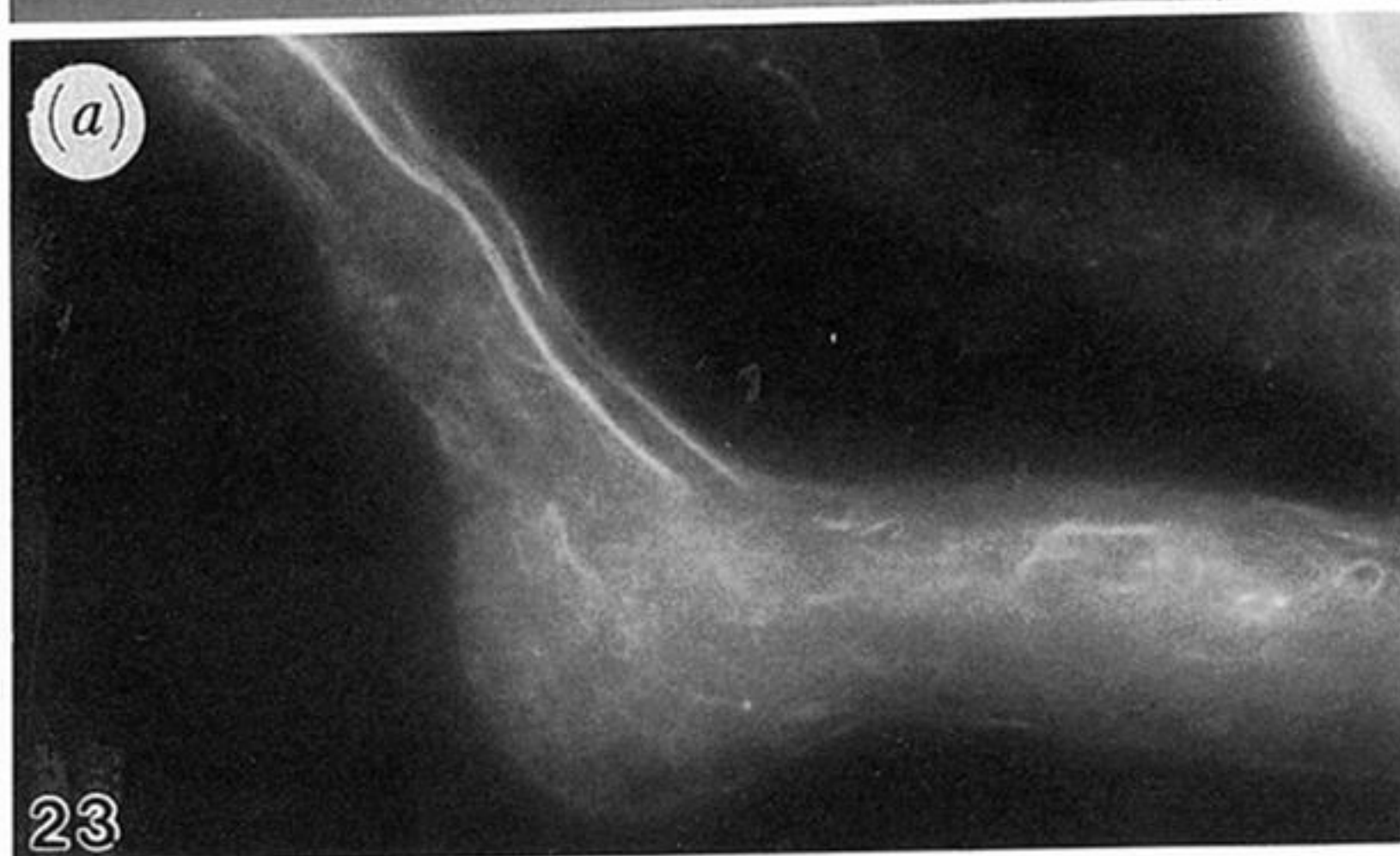
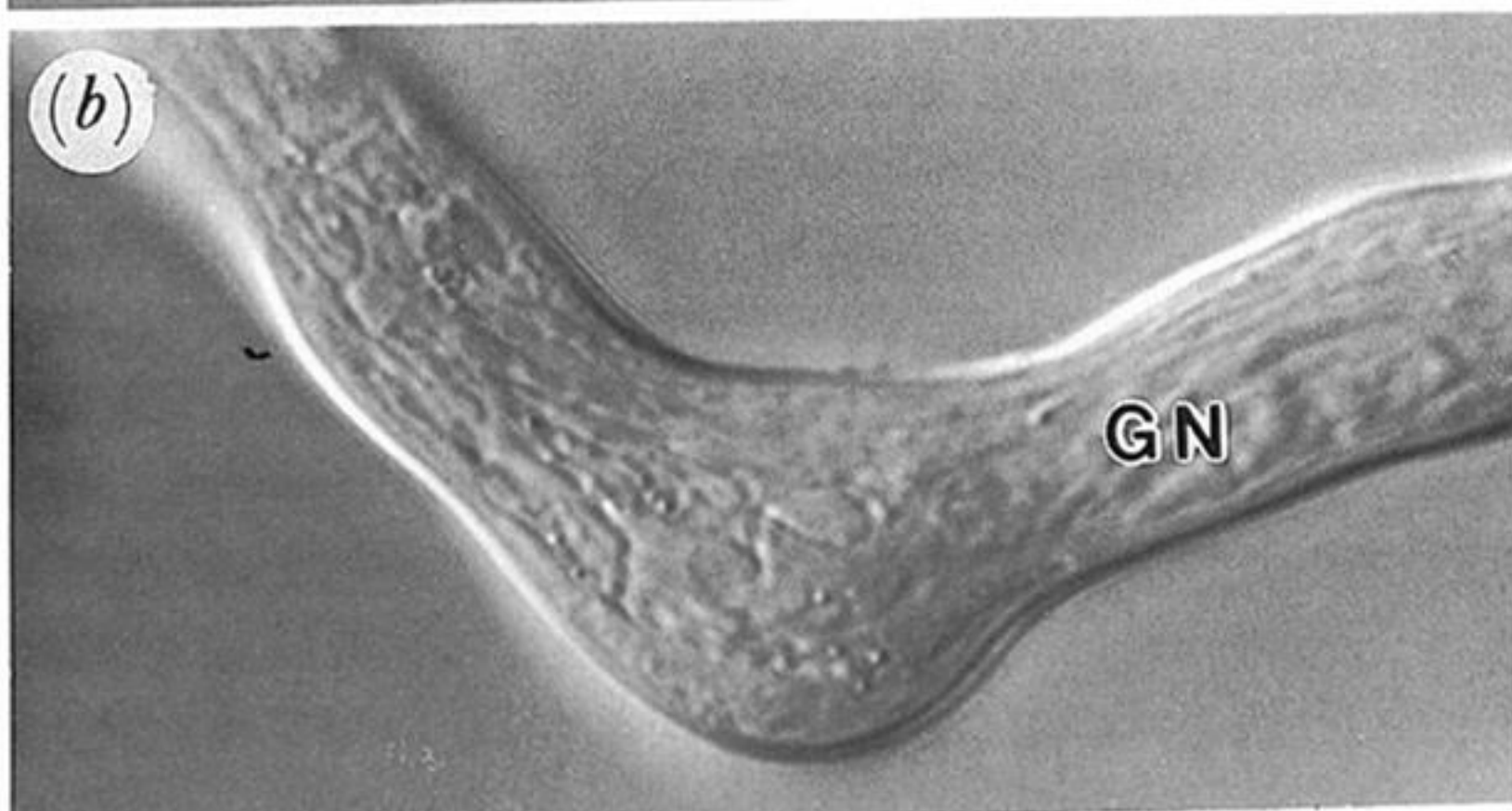
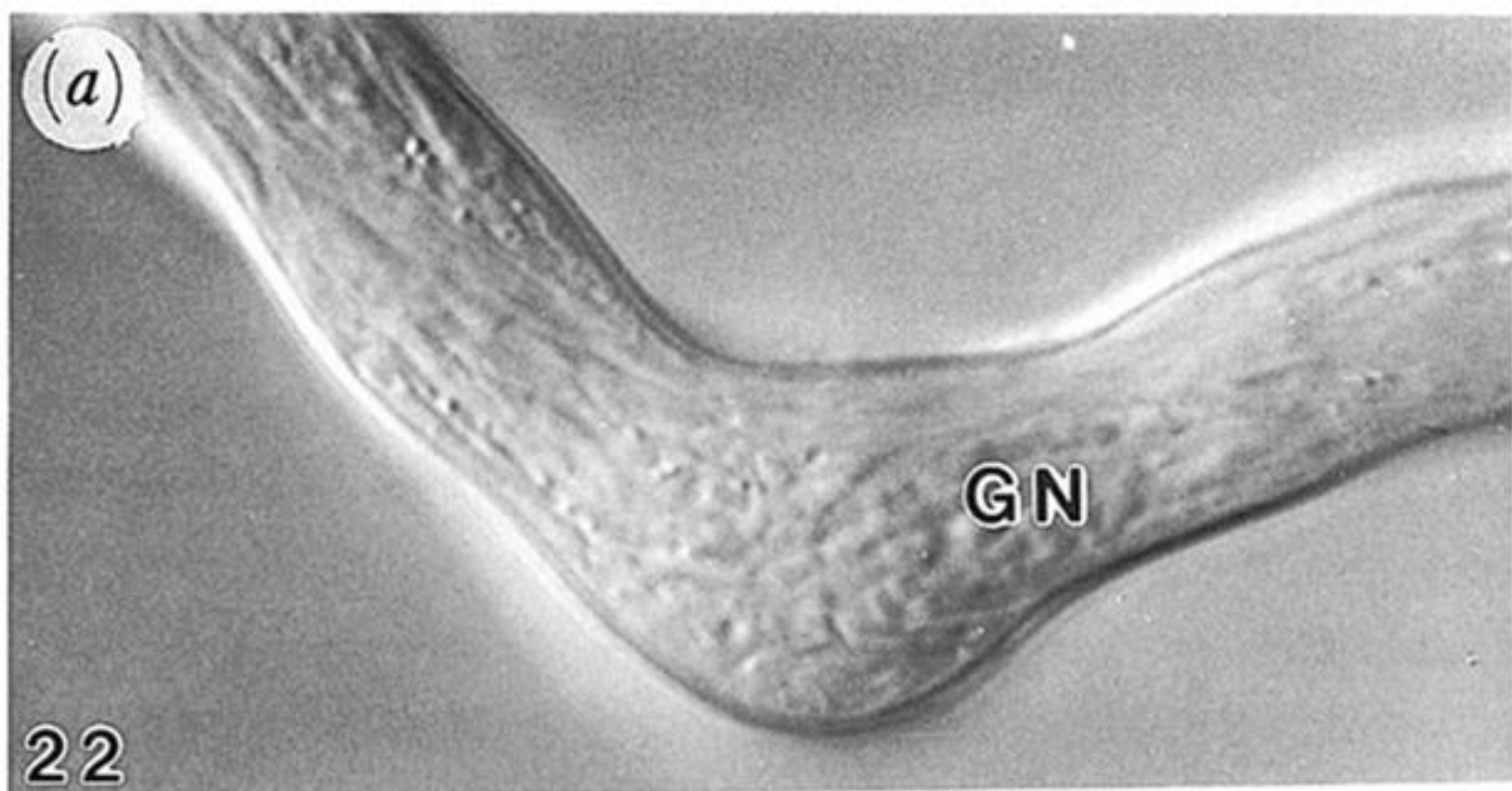


Figure 11. Swollen apex after 10 min recovery showing continuous wall thickening with occasional more massive wall thickenings (arrow head). Such thickenings are irregularly multilamellate and chemically heterogeneous (Heslop-Harrison *et al.* 1990*b*). Exposure 6 s. Figure 12. As figure 11. Movement was sluggish in this tube, and the generative cell (GC), in which chromosomes can be distinguished, had moved towards the apex. Exposure 3 s. Figure 13. As figure 11. The flow pathways in this tube, which was swollen asymmetrically, entered the apex, and in the focal plane of this micrograph appeared to encircle a central core containing a stranded group of lipid globuli and organelles. Exposure 6 s. Figure 14. Tube after 15 min recovery with an emergence possibly defining a prospective secondary apex. While the flow pathways were well defined in the tube and into the apical swelling, movement in the emergence was random. As in the tube of figure 13, particulate inclusions in the centre of the apical bulb were static during the period of the exposure. Exposure 6 s. Figure 15. Tube comparable with that of Fig. 14, viewed in a sequence of 3 planes along the axis of the prospective apex. All exposures 6–8 s. (a) Focal plane transecting the parent tube. The flow pathways are well defined, and in this focal plane seem to continue around the apical swelling. The static bodies in the centre include both lipid globuli, distinguishable by higher refractive index, and rod-shaped mitochondria. (b) Focal plane near the base of the prospective tip. Most of the inclusions at this level are identifiable as mitochondria. (c) Focal plane near the extreme tip, showing mitochondria and smaller unidentifiable inclusions. Figure 16. Swollen, thin-walled prominence produced by a tube during a recovery period of 20 min. The outgrowth appears to have formed following the disruption of the original wall, remains of which can be seen to the right (arrow head). The vegetative nucleus (VN) has moved into the new outgrowth. Exposure 3 s. Figure 17. Tube from the same sample as that of figure 16. The outgrowth in this case is completely surrounded by a collar of material derived from the original wall of the terminal bulb, in which the vegetative nucleus (VN) can be distinguished. The emergence is forming a new tube apex, with the first evidence of organelle zonation. Exposure 3 s.



Figures 18 and 19. Apical zones of pollen tubes of *Endymion nonscriptus* during recovery from 10 min exposure to medium containing $5 \mu\text{g ml}^{-1}$ CD. CFW staining for cellulosic glucans. (Magn. $\times ca.$ 830.) Figure 18. Initiation of a secondary apex; 10 min recovery period. Figure 19. Emergent secondary tube after the transition to cylindrical growth; 15–20 min recovery period.

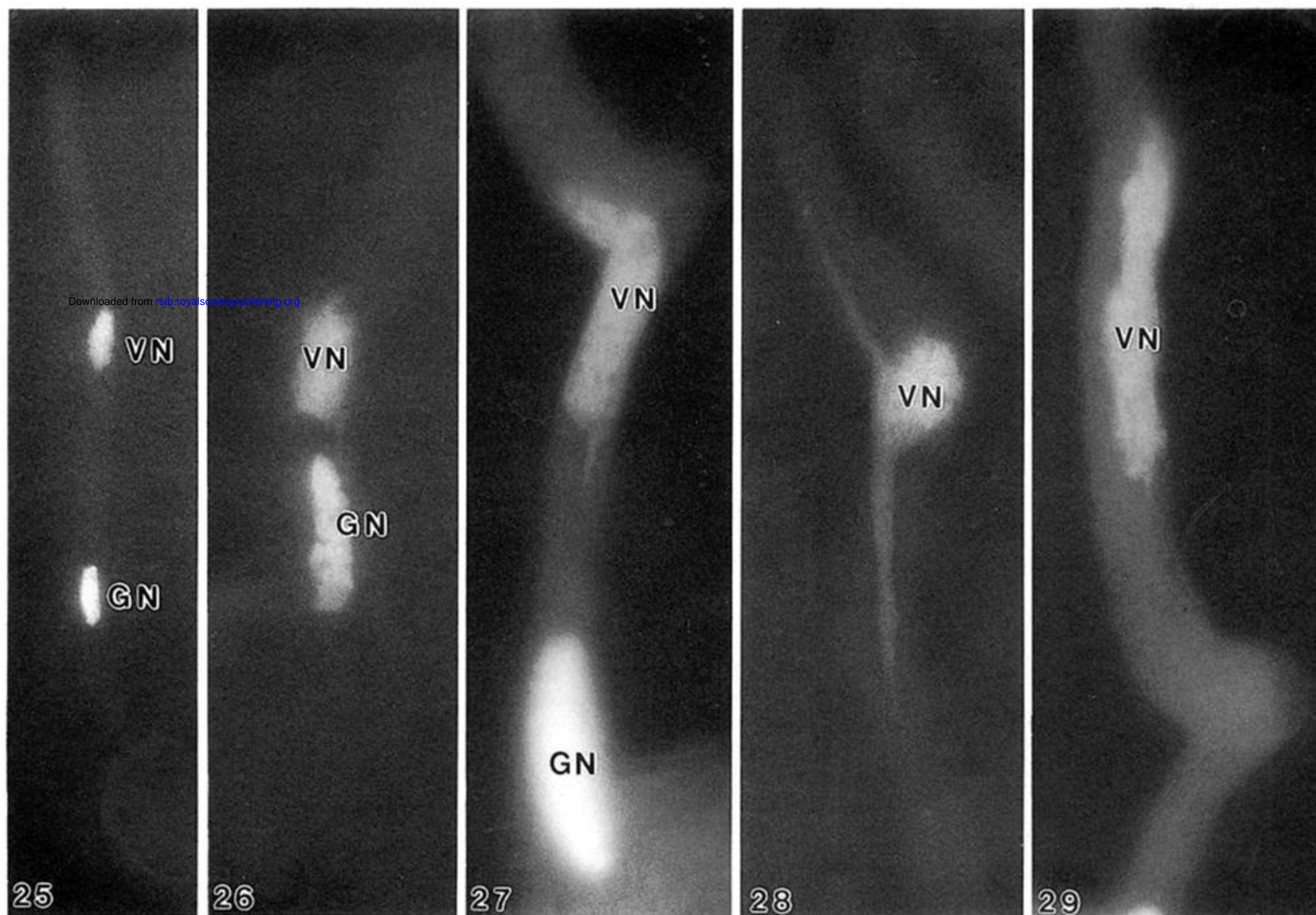
Figures 20 and 21. As for figures 18 and 19, DAB staining for callose. Figure 20. Tube after a 10-min recovery period with a thin-walled emergence, likely to mark the site of a prospective apex, to the right of the apical swelling. (Magn. $\times ca.$ 680.) Figure 21. Tubes from the same culture as that of figure 19. The upper of the pair has developed a secondary apex along the same axis as that of the parent tube, and is in the early stages of the transition to cylindrical growth, with a well-defined callosic sheath. The lower shows the more usual configuration, with the secondary tube, now in the cylindrical growth phase, having departed at an angle from the site of arrest. (Magn $\times ca.$ 794.)



Downloaded from rstb.royalsocietypublishing.org

Figure 22. DIC micrographs of living pollen tubes of *Endymion conscriptus*; 20 min recovery following 10 min in medium containing $5 \mu\text{g ml}^{-1}$ CD. (Magn. $\times ca.$ 1085.) The segment illustrated includes the swelling marking the site of arrest. The secondary tube has emerged and was extending actively at the time of the 3 s exposures. The principal flow pathways in the focal plane of the micrographs can be distinguished in both parent (left) and secondary (right) tubes, and also the tendency for moving bodies to follow the inner side of the bend, by-passing the residual swelling. (a) Generative cell (GN), identifiable by the chromosomes, at the site of the bend. (b) Same field *ca.* 4 min later, with the generative cell now moving through the secondary tube.

Figures 23(a) and (b). Segment of a tube comparable with that of figure 22 viewed in two focal planes. Tr-Ph staining; (Magn. $\times ca.$ 1085.) The actin fibrils extend around the inner side of the bend, defining the principal pathways of movement between the older (left) and newer (right) parts of the tube (*cf.* figure 22); none extends continuously through the residual swelling.



Figures 25–29. Pollen tubes of *Endymion nonscriptus* following 10 min in medium containing $5 \mu\text{g ml}^{-1}$ CD. DAPI staining for the nuclei of the vegetative (VN) and generative cells (GN). The tube tip is to the top of each micrograph. Figure 25 (Magn. $\times ca.$ 229); remainder magn. $\times ca.$ 615.) Figure 25. Disposition of VN and GN in a pollen tube from a culture comparable with that of figure 5, immediately following CD treatment. The VN is condensed along the length of the tube, and in this instance the VN leads the GN by $70 \mu\text{m}$. There are no persistent links between the vegetative and generative cells in this species. Figure 26. As figure 25, earlier stage of emergence of the generative cell and VN. The residual prominences on the latter mark the likely sites of former links to actin fibrils. Figure 27. Tube 70 min into recovery, VN entering the site of arrest and beginning to by-pass the CD-induced swelling. In this instance the diameter of the secondary tube was substantially greater than that of the original. Figure 28. As figure 27; VN delayed in the CD-induced swelling. Long pointed processes extend in both directions along the tube, indicating association with differently polarized elements of the actin cytoskeleton (Heslop-Harrison and Heslop-Harrison 1989*b*) and illustrating the great elasticity of the nuclear envelop. Figure 29. VN progressing through the secondary tube. The extended state is that to be expected in normal tubes of this age.